A Numerical Simulation of Warm Fog Dissipation by Electrically Enhanced Coalescence: Part I. An Applied Electric Field

PAUL M. TAG

Naval Environmental Prediction Research Facility, Monterey, Calif. 93940

(Manuscript received 15 April 1975, in revised form 2 December 1975)

ABSTRACT

It has been suggested that the use of charged particles or electric fields be considered as a technique for dissipating warm fogs. The study presented here attempts to determine the degree of improvement one could expect as the result of one aspect of electrically enhanced coalescence—enhanced coalescence due to an externally applied electric field on neutral drops. For this purpose, a numerical simulation with a one-dimensional microphysical fog model which incorporates the process of collision-coalescence was conducted. Collision efficiencies appropriate to two extreme electric fields were utilized for the numerical experiments. It was determined that a noticeable improvement in visibility can be achieved only under extremely large field strengths, and then only for certain fog spectra.

1. Introduction

Several techniques for improving the visibility in a warm fog have been suggested and tried in field experimentation. Thermal dissipation, treatment with hygroscopic materials, and helicopter downwash have been predominate among those both theoretically and experimentally studied. Utilization of electrostatic effects has been suggested as still another possibility.

The idea that electrical fields and charged droplets can modify the microphysical state of a cloud or fog is not a new one. Lord Rayleigh (1879) noted the affect of static electricity on the spray of droplets from a water jet and even suggested a possible connection between rain formation and electrical effects. Pauthenier (1950) was one of the first to suggest that seeding with charged drops might be a viable technique for clearing a fog. However, due to the realization that the onset of precipitation in a warm cumulus cloud is much dependent on the speed with which small droplets grow, many of the initial theoretical and laboratory studies were done with clouds in mind. Cochet (1952) addressed the problem of cumulus cloud modification and concluded that treatment with charged water drops could accelerate the microphysical process of coalescence.[1] Sartor (1954), also recognizing the importance of coalescence in natural cumuli, conducted laboratory investigations into the affect of an electric field on collection efficiencies. He found that coalescence of droplets in the 5–25 μm radius range was increased significantly with the application of a parallel electrostatic field. Goyer *et al.* (1960) later conducted similar experiments with larger drops. Several studies in the 1960's (e.g., Sartor, 1960; Lindblad and Semonin, 1963; Plumlee and Semonin, 1965) demonstrated, theoretically, that collision efficiencies are increased by the presence of an electric field.

More recent work has rejuvenated the concept of fog clearing by using electrostatic effects. However, a difference of opinion exists as to what mechanism would, in fact, be responsible for creating a change in the microphysical fog structure. As suggested by the above discussion, one would assume that enhancement of coalescence is that mechanism. Smith (1972), in considering fog dispersal by seeding with charged drops, emphasized this effect. Gourdine *et al.* (1974), however, developed a fog modification system involving charged droplets, but proposed an alternate mechanism—field-induced precipitation. They postulated that, after being inserted above and through the fog, charged droplets attach themselves to fog droplets and precipitate out in response to the electric field created by the charged droplets. Although this effect may play a part, this study will address only enhanced coalescence.

Enhanced coalescence must be thought of with respect to two effects. One is the result of neutral fog droplets immersed in an externally applied field. A vertically oriented field polarizes all droplets, resulting in charges of opposite sign on the tops and bottoms of all drops. The second effect results from charges on individual drops. Charged drops polarize others nearby, thus again resulting in enhanced collision efficiencies. Carroz *et al.* (1972) made an initial attempt at determining visibility improvement as the

[1] In the title of this paper and in this usage, "coalescence" is a shortened way of saying collision-coalescence. Any specific meaning of the term coalescence will be noted.

result of this effect, but considered only monodisperse fog and treatment droplets in conjunction with a continuous growth process for the charged drops.

It is the purpose of this study to investigate both of the above effects. Part I will consider only enhanced coalescence of neutral drops due to an externally applied field. This investigation is based on a numerical simulation of this effect and a determination of visibility improvement in response to several magnitudes of field strength. It is recognized that the electric fields that will be simulated are extreme and would be operationally difficult to produce, at least over the depth of fog that will be considered. However, it must be remembered that the purpose of this study is to examine one mechanism that has been postulated to be important. Should this mechanism prove ineffective even for extreme field strengths, future efforts should then not emphasize such an effect.

It is also recognized that an isolation of one mechanism is a gross simplification of an experimental situation. The other mechanisms cited above are undoubtedly active simultaneously. Differential settling of neutral droplets in an electric field, for example, leads to droplet charging (Sartor and Abbott, 1968). The complexity of the numerical simulations, however, in addition to complications arising from interactions of the processes, suggests an isolation of the mechanisms.

2. Model description and numerical procedure

a. Basic model description

Because the effect noted above is primarily a microphysical one, a primarily microphysical model was developed for this study. No attempt is made at predicting the onset of fog or allowing for fog formation processes. Instead, an empirical droplet spectrum is used to initialize the computations. Recognizing that collision-coalescence produces even larger drops which become more efficient collectors as they fall, it was considered important that the model be a multi-leveled one. For this purpose, the model has 10 levels in the vertical. After initially prescribing a fog droplet spectrum at each of these levels, the processes of stochastic coalescence and vertical transfer of droplets by droplet fallspeed plus turbulent mixing then cause changes in the spectra. Visibility is then computed from these spectra.

b. The differential equation

Let $N(r,z,t)$ be the average number of droplets of radius r, at a height z, and time t. The partial differential equation which then describes the processes given above is

$$\frac{\partial N(r,z,t)}{\partial t} = -w(r)\frac{\partial N(r,z,t)}{\partial z} + \frac{\partial}{\partial z}\left[K\frac{\partial N(r,z,t)}{\partial z}\right] + Q(r,z,t), \quad (1)$$

where $w(r)$ is the terminal velocity of a droplet of radius r, K the eddy exchange coefficient, and Q a source/sink term to account for collision-coalescence. Explicit finite-difference schemes are used for the advective (forward in time, backward in space) and turbulent diffusion (forward in time, centered in space) terms. All experiments were run for 30 min of model time, using a time step of 5 s.

In the solution of (1), no mixing of droplets into the free air above the fog is permitted. Similarly, mixing of droplets from level one into the ground does not occur. Droplets must fall from the fog in order to be removed from the system. This latter restriction prohibits any visibility improvement from occurring there as the result of turbulent mixing, a mechanism not, in itself, being examined here.

c. Droplet categories

The process of stochastic coalescence, operating on only a small initial number of different sized drops, by definition, results in a myriad of new size combinations after just several time steps. It would be physically difficult to keep track of all combinations for very long. As a result, and as is commonly done, Eq. (1) is solved at each of the 10 levels for a sequence of fixed radii. For the process of coalescence, newly created droplets are refit back into the fixed discrete sizes. The fitting procedure will be described in the following section.

As suggested by Berry (1967), a logarithmic size sequence is used. Such a sequence allows good resolution at the smallest sizes where it is generally needed, but also permits inclusion of the larger precipitation-size drops if they should be required. A simple multiplicative radii sequence, based on a constant factor γ, was chosen, i.e.,

$$r_{j+1}=\gamma r_j,\ r_{j+2}=\gamma^2 r_j,\ \text{etc.} \quad (2)$$

The subscript j designates droplet category, and r_1, the smallest radius, is 1 μm.

Eq. (3) describes a desirable criterion for γ:

$$r_j^3+(r_{j+1})^3<(r_{j+2})^3 \quad (3)$$

or

$$r_j^3+(\gamma r_j)^3<(\gamma^2 r_j)^3.$$

Such a restriction allows no droplet size combinations (resulting from coalescence) to advance past one category greater than the largest of the two combining

droplets. The smallest two-place value for γ which will satisfy this inequality is 1.18. Consequently, we arrive at a numerical sequence of radii: 1.00, 1.18, 1.39, 1.64, etc. In this study, only droplet categories for sizes up to several hundred microns were necessary.

d. Coalescence of droplets

The important relevant process simulated in this study is collision-coalescence, the term Q in Eq. (1). For a given level and time, the change in droplet number due to stochastic coalescence, as used by Kovetz and Olund (1969), may be written

$$Q(r_i)\Delta t = -N(r_i)\sum_{n=1}^{i-1} P(i,n)B(i,n) - \sum_{n=i+1}^{M} N(r_n)P(n,i) + N(r_{i-1})\sum_{n=1}^{i-2} P(i-1,n)B(i-1,n), \quad (4)$$

where i and n both refer to category numbers, and M is the total number of categories. $P(i,n)$ is defined as the probability that an ith droplet will collect an nth droplet in time Δt:

$$P(i,n) = V(i,n)N(r_n)\Delta t, \quad (5)$$

where $V(i,n)$, as defined by Berry (1967), is the collection kernel

$$V(i,n) = \pi r_i^2[Y_c(r_i, r_n)]^2 E[w(r_i) - w(r_n)]. \quad (6)$$

In (6) Y_c is the linear collision efficiency as used by Shafrir and Neiburger (1963) and E the coalescence (as opposed to collision) efficiency. The mathematical approximations of Wobus *et al.* (1971) are used for the droplet terminal velocities $w(r)$.

The partitioning scheme is that of Kovetz and Olund (1969) who utilized the partitioning factor B to ensure that both mass and number are conserved:

$$B(i,n) = \frac{(r_i^3 + r_n^3) - r_i^3}{r_{i+1}^3 - r_i^3} = \frac{r_n^3}{r_{i+1}^3 - r_i^3}. \quad (7)$$

Eq. (4) is solved for category numbers $i=3$ to $i=M-1$ (categories 1, 2 and M must be considered separately) and allows for all combinations of collisions that either increase or diminish the number of droplets in a category. The number of r_i particles decreases as a consequence of collisions with larger particles, and as a consequence of partitioning of liquid water between r_i and r_{i+1} because of collisions of r_i droplets with smaller droplets. The number of r_i droplets increases as the result of partitioning between r_{i-1} and r_i because of collisions of r_{i-1} with smaller droplets. By utilizing the criteria imposed by Eq. (3), there is no danger of droplets entering a category from sources other than those described above.

The accuracy of the partitioning scheme [Eq. (7)] was tested by comparing numerical solutions to analytic solutions generated both from the sum of masses kernel of Golovin (1963) and the constant kernel of Scott (1968). As noted by Berry and Reinhardt (1974), who had examined this particular scheme, it was found that a pseudo-diffusion of droplet

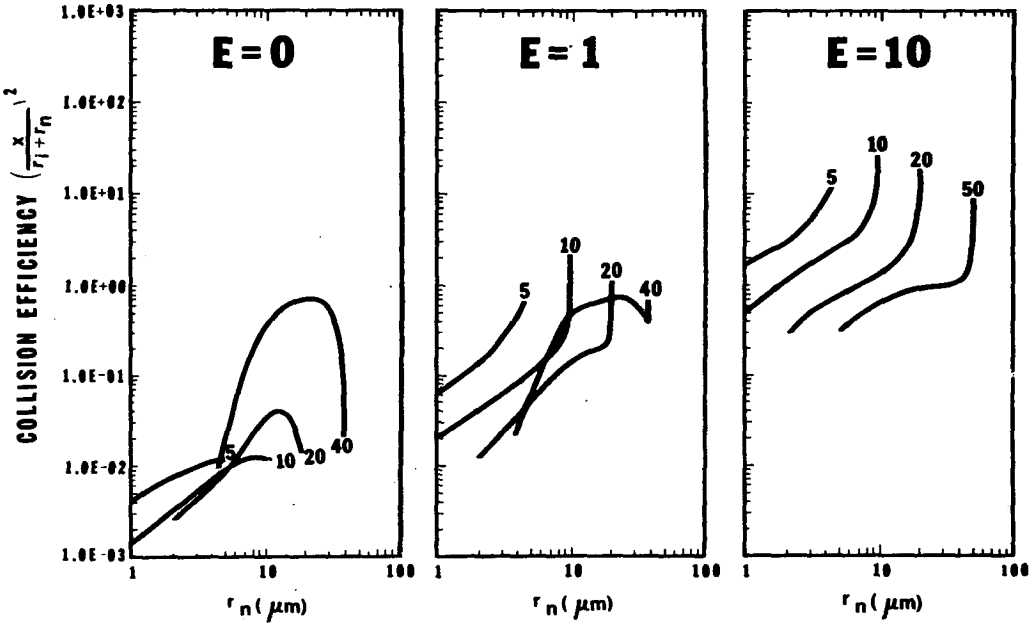

FIG. 1. Collision efficiencies for several collector drop radii (μm) for electric fields of 1 and 10 esu cm^{-1}, compared to normal hydrodynamic efficiencies for no field [x specifies the critical trajectory, as defined by Fletcher (1962)].

mass resulted in a solution that was slightly "fast." Such an inaccuracy would be significant if the absolute magnitude of the results presented in this paper were important. Since the point of this study is to make a relative comparison between collection kernels, both with and without the effect of an electric field, the inaccuracies of the scheme become less important.

In numerical models of the type being described, the coalescence efficiency (that fraction of collisions which results in actual merging) is usually set equal to 1. Recent evidence indicates that such might not be the case (Whelpdale and List, 1971; Levin *et al.*, 1973). Sartor (1954, 1960) concluded, however, that coalescence (as opposed to collision) is aided in the presence of electric fields and that with very strong fields all collisions would result in coalescences. For this reason, a coalescence efficiency of 1 is used for the electric field simulations. For consistency, and because nonfield coalescence efficiencies are not completely understood, a value of unity will likewise be used for the "control" situations.

e. The collection kernel

In order to add the effects of an electric field to a numerical model of collision-coalescence, modifications must be made to the normal hydrodynamic collection kernel given in Eq. (6). Assuming that the coalescence efficiency can be set equal to 1, an external electric field applied to electrically neutral fog droplets results in alterations only to the collision efficiencies of the kernel.

The mathematical simulation of the movement of two interacting bodies is a complicated one. The equations of motion of the particles must be solved with all of the important forces affecting the movement. Sartor (1960) was one of the first researchers to incorporate electrical forces into these equations. Lindblad and Semonin (1963) and Plumlee and Semonin (1965) also made efficiency calculations for various fields. Paluch (1970) was able to produce several analytic approximation formulas for certain ranges of charged droplets with no field, and large charged drops with a field, but not for neutral droplets in a field.

In an attempt to acquire collision efficiencies for several extreme field strengths, Dr. J. Doyne Sartor of the National Center for Atmospheric Research was contacted. Dr. Sartor described the cases for which he had computer runs from their numerical model ORACLE, a very elaborate droplet trajectory model which includes the effects of electrostatic forces [based on work by Davis (1964) and Davis and Sartor (1967)]. He kindly offered to forward the collision efficiencies for two extreme field strengths, fields of 1 and 10 electrostatic units (esu) cm^{-1} (3×10^4 and 3×10^5 V m^{-1}, respectively). Efficiencies for these two fields for several collector drop sizes, along with the normal hydrodynamic ones, are shown in Fig. 1.

For the 1 esu cm^{-1} electric field, the efficiencies approach the normal hydrodynamic ones after the collecting drop exceeds ~30 μm radius. Similarly, for $E=10$ esu cm^{-1} the electric field is negligibly felt beyond ~50 μm radius. Consequently, for sizes larger than those limits, the normal hydrodynamic efficiencies, calculated from the numerical fits by Berry (1967) of the Shafrir-Neiburger collision efficiency curves (1963), are used. Because the Berry approximations are not valid for small droplet radii, hydrodynamic efficiencies for sizes <28 μm (for the control case where the field is zero) are based on the calculations of Davis and Sartor (1967). All efficiencies are calculated or read in at the start of the model run and stored for later use.

f. Visibility calculations

Since the primary goal of fog modification is the improvement of visibility, the visibility calculation, as a function of the droplet spectrum, is a very necessary and important part of the model. By incorporating the contributions of all droplet categories (at one level at a given time), visual range (VR) can be calculated from

$$\mathrm{VR}=1.245\left[\sum_{i=1}^{M} N_i r_i^2 (K_s)_i\right]^{-1}, \tag{8}$$

where K_s is the scattering coefficient. Johnson (1972) has provided a review of the derivation of Eq. (8), together with the computer subroutines necessary to calculate the scattering coefficient as a function of droplet radius. As noted by Jiusto (1974), it is not adequate to assume the scattering coefficient to be equal to a constant.

g. Limitations of the model

The one-dimensional model used for this study effectively assumes a horizontal uniformity both of the fog structure and of the modification mechanism. In any fog dissipation experiment one encounters the difficulty of untreated fog advecting or mixing in from the sides of the treated area. Such replenishment obviously diminishes treatment effect. A similar problem exists if fog formation processes are at work. The one-dimensional model just described has none of these counteracting effects. Consequently, a visibility improvement predicted by the model should be interpreted as an overestimate.

Although a two-dimensional model which incorporates horizontal influences could have been developed, the accompanying time and computer expenditures did not seem to justify such an approach. The philosophy behind the current one-dimensional model is

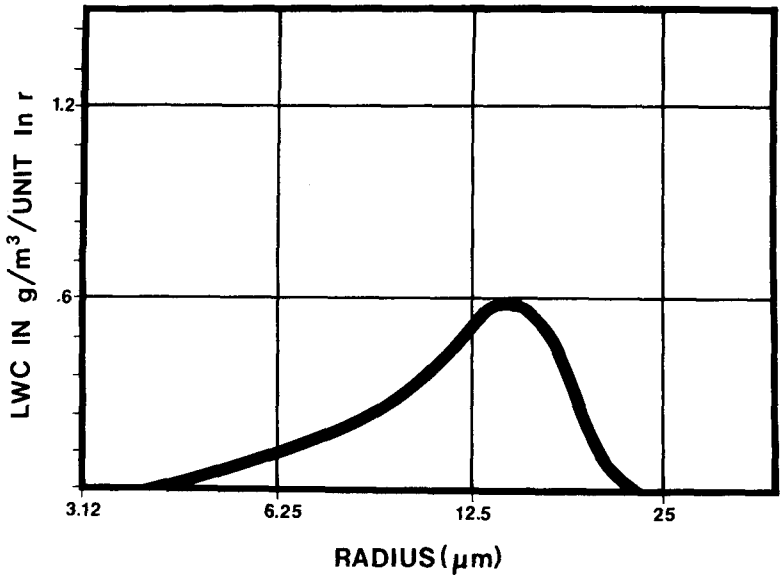

FIG. 2. Initial fog droplet mass distribution used in model experiments (LWC = 0.39 g m^{-3}).

to provide guidance by way of relative effect. The real utility of the model is seen in its ability to compare an electric field simulation to a control and thus to evaluate the potential of the mechanism being simulated here.

3. Initial fog conditions

A fog droplet spectrum or distribution must be specified at each of the model's 10 levels to initiate computations. Fog spectra vary widely from one fog type to another and even from one to another of the same type. Consequently, two spectra representing two extremes of spectral width and droplet size are used. The water mass spectrum which is used for most of the model experiments is shown in Fig. 2 and is based on data taken in the radiation-drainage type fogs of the Panama Canal Zone, a fog previously studied from the standpoint of hygroscopic seeding (Tag, 1971). A more continental spectrum with smaller droplet sizes will be considered later. Fig. 2 represents a spectrum with a mean volume radius of 10.8 μm, a liquid water content of 0.39 gm m^{-3}, and produces a calculated visibility of 143 m. Fog in the Canal Zone is typically between 100 and 200 m in depth. Choosing a model depth of 150 m results in a grid spacing of 15 m.

An appropriate exchange coefficient is necessary for the diffusion computations. Smith *et al.* (1970) made estimates of exchange coefficients in several California fogs. Based on aerial measurements of turbulence, coefficients ranged from 1–10 m^2 s^{-1}. A choice of 2 m^2 s^{-1}, a value nearer the lower end of the spectrum, was arbitrary chosen for the numerical experiments.

4. Results of the model experiments

a. Electric field vs no field

Using the conditions specified in Section 3, three experiments were run to test the relative effect of the two electric fields. All three cases utilized the fog distribution discussed in Section 3. Case I was a control and was run with the normal hydrodynamic collection kernel for the full 30 min. Cases II and III utilized the kernels appropriate for fields of $E=1$ and 10 esu cm^{-1}, respectively.

The results generated by the control case are shown in Fig. 3 where visibility and liquid water content (LWC) vs height are plotted for 10, 20 and 30 min model time. Note that visibility at $t=0$ is 143 m at each of the 10 model levels. As expected, there is minimal improvement in visibility. LWC decreases slightly at all model levels as the result of preferential fallout of larger particles. Only in the upper regions of the fog (because of non-replenishment of droplets from the clear air above level 10) does a visibility change accompany LWC decrease. Obviously, large particles which have fallen from the lower half of the fog do not significantly restrict visibility. Although LWC can generally be related to visibility, these two parameters are not related perfectly since visibility is also a function of the droplet size distribution.

Case II, for a field of 1 esu cm^{-1}, showed little improvement over the control; the results are not shown here. Slightly more water falls from the fog because of enhanced growth, but the visibility improvement accompanying this decrease is minimal.

Fig. 4, for an order of magnitude larger field (10 esu cm^{-1}), depicts an identifiable change. The visibility

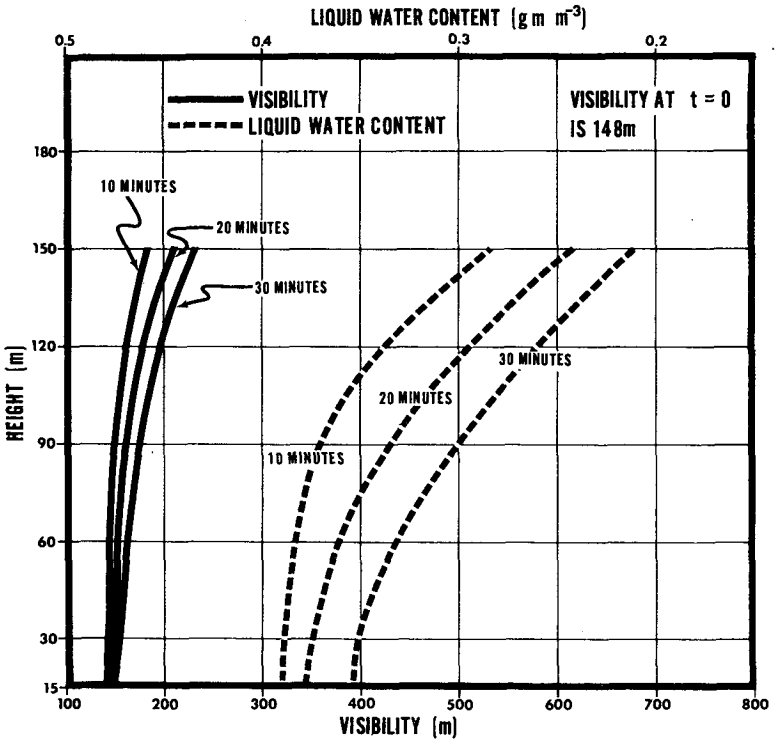

FIG. 3. Variation of visibility and liquid water content for Case I (E=0 esu cm^{-1}).

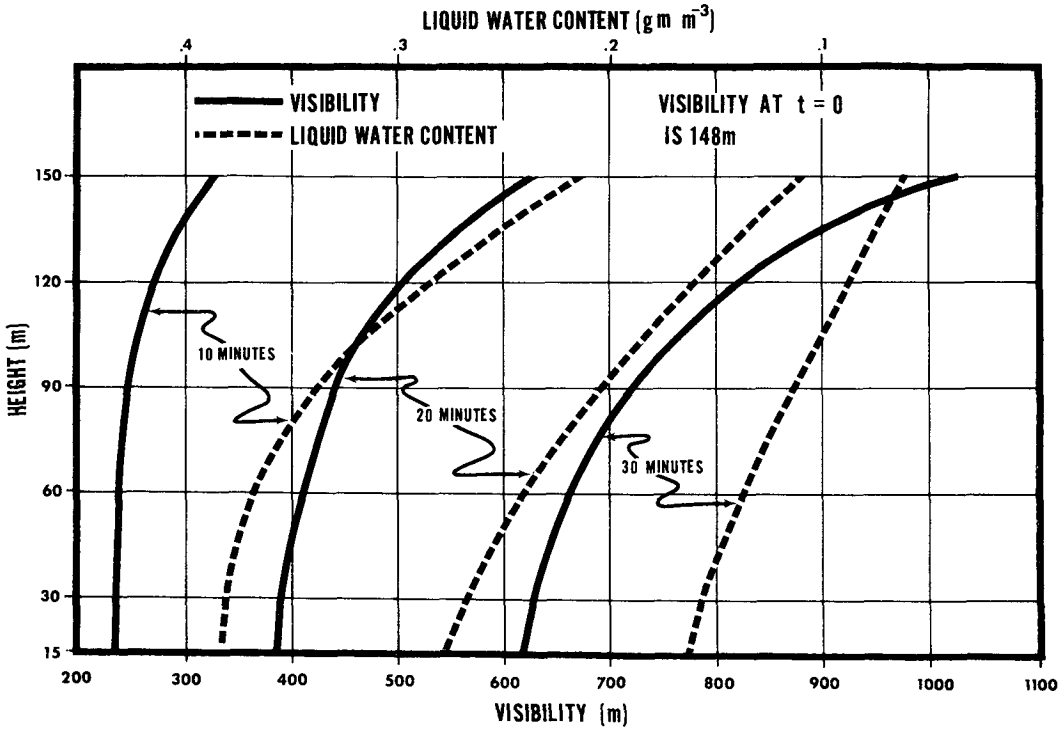

FIG. 4. Variation of visibility and liquid water content for Case III (E=10 esu cm^{-1}).

improvement factor (VIF), which is defined as the visibility after 30 min divided by the initial visibility, gives a measure of the degree of improvement. Whereas the VIF's for both the no-field fog and the $E=1$ esu cm^{-1} case barely surpass 1.5, the VIF's for Case III vary from 4.3 at the lowest model level to 7.2 at fog top.

A visual presentation of the effect of the collection kernel and thus of the effect of the mechanism at work here is presented in Fig. 5 for Case III. Droplet mass spectrum evolution is shown for alternate levels of the model. The height of each spectral curve is a measure of the liquid water content and the slant axis the radius of droplet. The figures for Cases I and II (not shown) showed almost no perceptible movement of droplet mass. Consequently, the visibility improvement is small because very little droplet mass is transferred into sizes with non-negligible terminal velocities. In Case III ($E=10$ esu cm^{-1}), droplets do grow substantially and consequently inherit significant terminal velocities, resulting in the visibility improvement depicted in Fig. 4. Along with Cases I and II, this increase in mean droplet radius for the lowest level of the model is shown in Fig. 6. Although partially a result of the spectrum shift by itself (less light scattered by larger droplet sizes),

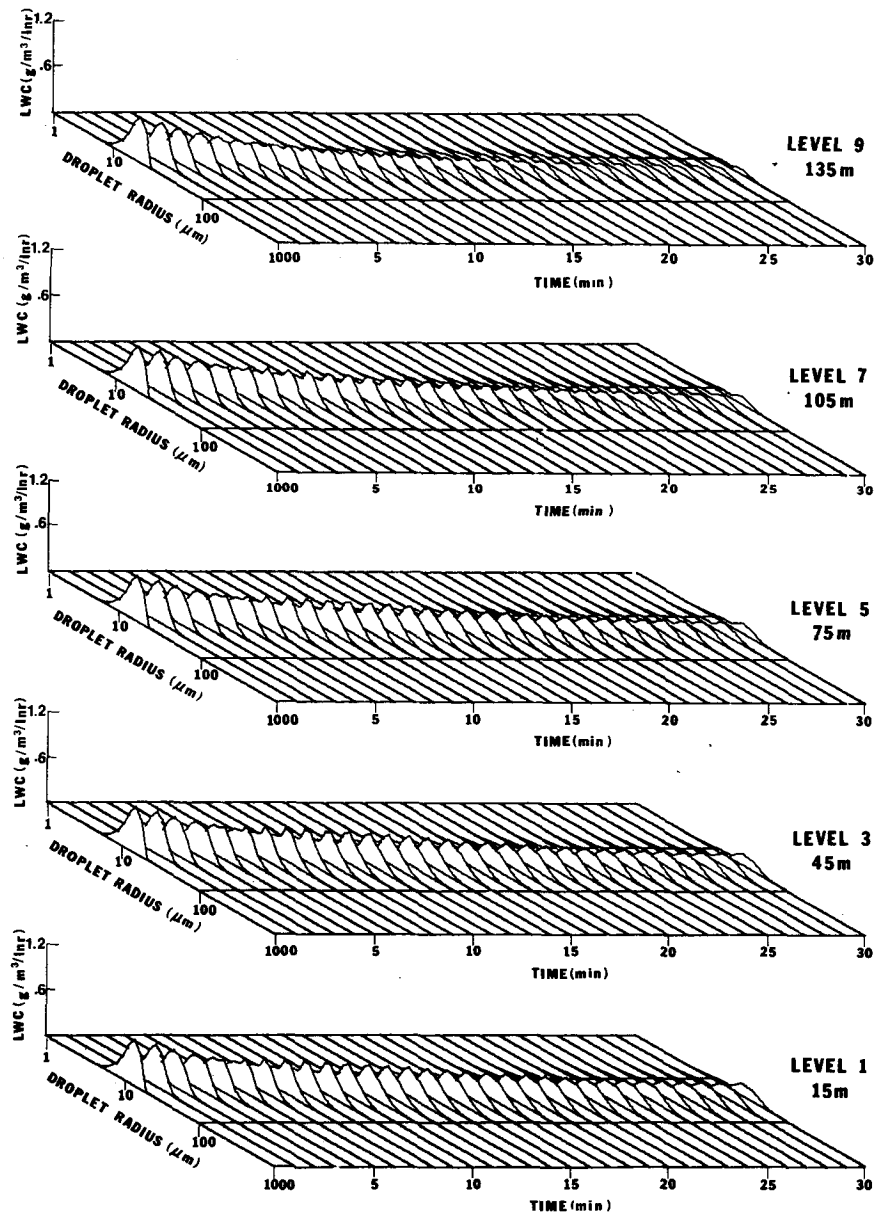

FIG. 5. Water mass distribution as a function of height, time and droplet radius, for Case III, $E=10$ esu cm^{-1}.

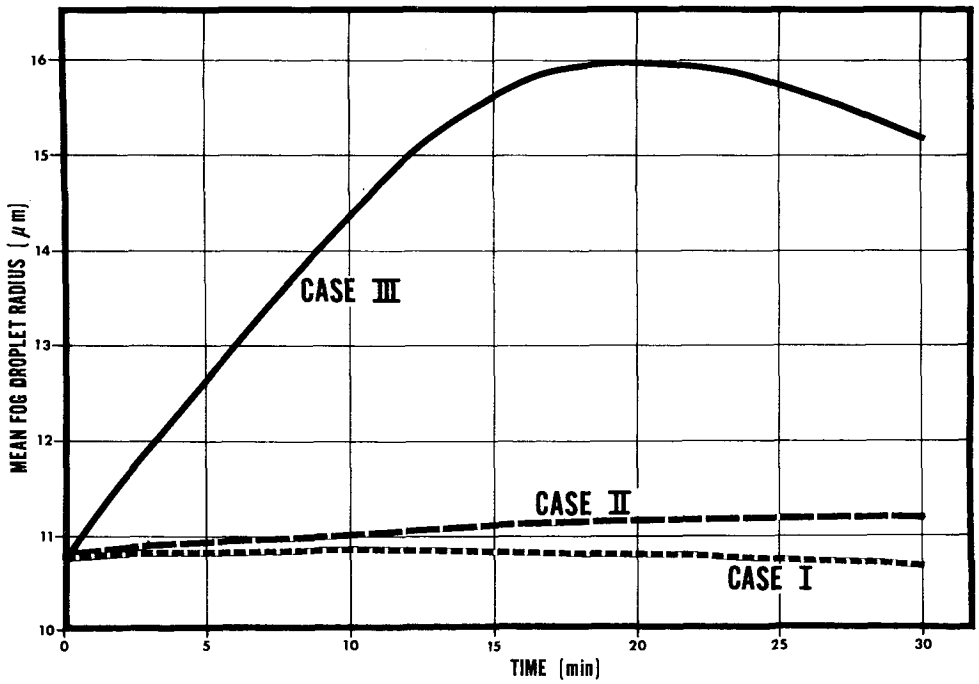

FIG. 6. Change in mean spectral droplet radius for level 1 as a function of time for Cases I, II, and III.

most of the visibility improvement here is the result of decreased droplet concentrations because of droplet fallout. This conclusion is reached if one compares the droplet shift at fog top to that shown in Fig. 6 for level 1 of the model. For Case III, even though the maximum droplet shift (of the mean of the total distribution) at level 10 is only 27% of that at level one, the VIF there is 75% larger. As seen in Fig. 4, the liquid water content is correspondingly smaller.

b. The effect of fog density

A fourth experiment was conducted to determine the effect of fog density on visibility improvement. Collision-coalescence should function more efficiently when the number density is larger. To determine the absolute effect on visibility improvement, Case III (10 esu cm^{-1}) was rerun with only one-third the liquid water content (0.13 g m^{-3}). The percentage frequency of droplet number remained the same.

The resultant visibilities and corresponding liquid water contents for Case IV are shown in Fig. 7. Although the absolute visibilities after 30 min are approximately the same as those for the 0.39 LWC fog, it must be noted that the initial visibility for Case IV is 428 m. Consequently, the VIF's for fog top and bottom are only 3.0 and 1.8, respectively—as opposed to 7.2 and 4.3 in Case III. Assuming that the initial droplet distribution is the same, the visibility improvement factor decreases with decreasing LWC.

c. The effect of the fog spectrum

It was originally felt that differences in the fog droplet spectrum would make little difference with respect to relative visibility improvement. However, experimentation with a second fog spectrum demonstrated that such is not the case. A spectrum having an identical shape as that in Fig. 2 but with droplet radii ranging from 1 to 7 μm with an LWC of 0.1 g m^{-3} is used for comparison. This distribution results in a mean radius of 2.9 μm and a calculated visibility of 77 m. Such a narrow spectrum with small droplets is representative of continental fogs as seen in the San Joaquin Valley of California (Reinking, 1975).

Comparison runs were made with the same electric fields as considered in Cases I, II and III. Surprisingly, maximum VIF's for the $E=10$ esu cm^{-1} case never exceeded 1.3 throughout the fog! Obviously, the initial droplet spectrum is very important. Variation of LWC for this spectrum verified the conclusion reached earlier in Subsection 4b. However, an increase to the LWC used in the previous fog spectrum, although successful in improving the VIF, resulted in deterioration to the absolute visibility since the initial visibility decreases with increasing LWC.

d. Discussion

One might have suspected that, prior to conducting these numerical simulations, the substantial increase in collision efficiency caused by application of an

electric field would result in a more impressive visibility improvement. Particularly for the 10 esu cm^{-1} field, efficiencies are often one to two orders of magnitude greater than corresponding hydrodynamic efficiencies. A closer look, however, shows that the effect of the field decreases quickly with increasing droplet size. Electrostatic efficiencies are only minimally different from hydrodynamic ones beyond 40 μm radius. Rapid growth diminishes rather quickly. More importantly, the capacity of these larger drops to remove smaller, visibility-restricting sizes is limited to little more than that of a collector with no associated electric field. On the other hand, in the case of the smaller droplet fog considered in Subsection 4c, growth is not limited by a reduction in the impact of the electric field. Maximum radii never exceed 25 μm. The 30 min time period simply does not permit sufficient growth. Neither is sufficient water transferred into less visibility-restricting sizes nor, more importantly, into sizes with substantial fall velocities.

5. Conclusions and implications

The following conclusions were drawn from the modeling experiments:

1) Extreme fields are necessary to produce a noticeable improvement in visibility.

2) Visibility improvement is strongly dependent on the initial fog liquid water content. Given the same droplet frequency distribution, the visibility improvement factor increases with increasing liquid water.

3) Visibility improvement decreases sharply with the average droplet size of the fog spectrum.

4) Visibility improvement is primarily a result of increased droplet fallout caused by spectral widening.

It is felt that, at least for electric fields no larger than 10 esu cm^{-1}, electrically enhanced coalescence as the result of an applied electric field alone is not an effective mechanism for clearing warm fog. For fog spectra with small droplet radii, as found in the valley fogs in California, visibility improvement is negligible. For larger droplet fogs, modest visibility improvements are possible, but require too long a period to be either useful or, considering an operational area with finite boundaries, attainable.

This report has investigated only one aspect of electrically enhanced coalescence. The effect produced as the result of charges on individual drops must also be studied. Visibility improvement resulting from an electric field alone has been shown to be unimpressive. Part II, which will consider enhanced coalescence as the result of seeding with charged drops, will provide a more complete evaluation of electrically enhanced coalescence as a potential mechanism for clearing fog.

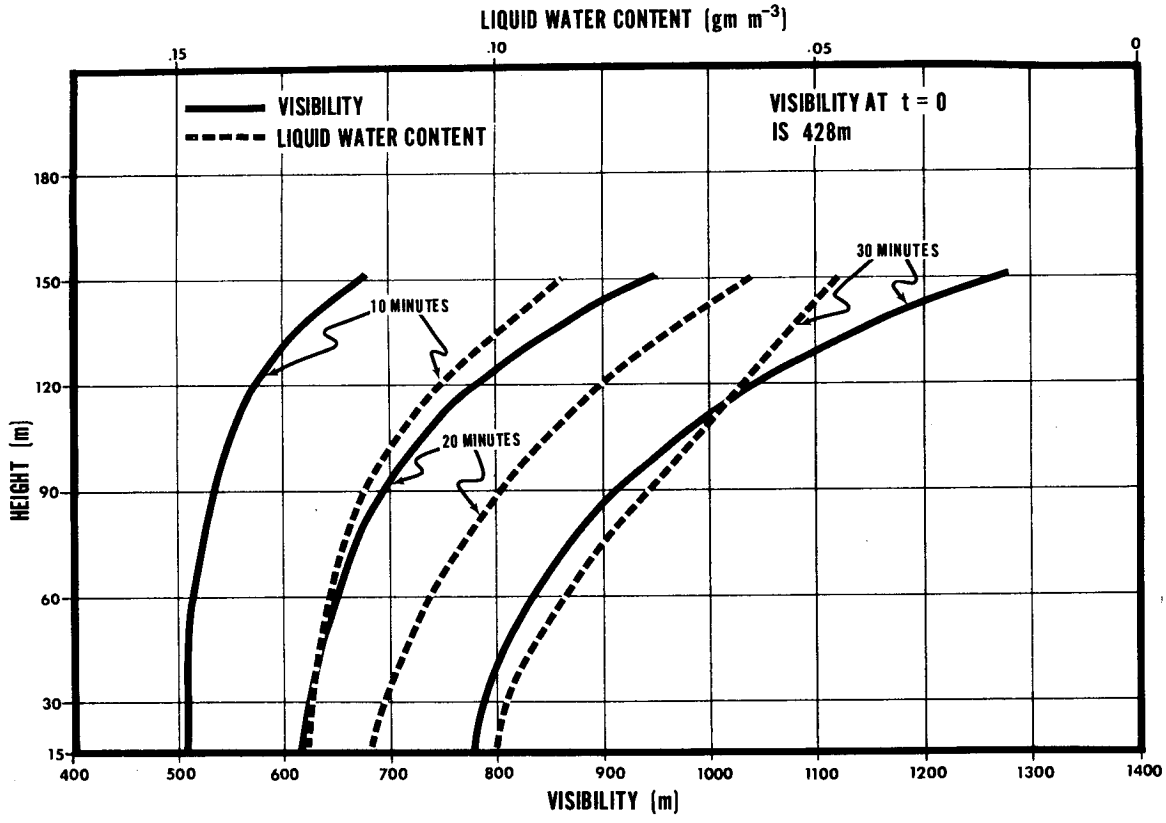

FIG. 7. Variation of visibility and liquid water content for Case IV ($E=10$ esu cm^{-1}).

Acknowledgments. I wish to express my appreciation to Mr. Paul Lowe who provided critical guidance during various phases of this study. Thanks must also go to Mr. Ken Richards who reviewed the manuscript, Mr. Milt Spritzer who assisted greatly in computer applications, Mr. David Johnson who provided computerized graphic aids, Mr. Richard Clark who drafted the figures, and Mrs. Linda Berkebile who typed the manuscript.

Special thanks must go to Dr. J. Doyne Sartor at the National Center for Atmospheric Research who provided necessary data without which this study could not have been accomplished.

REFERENCES

Berry, E. X, 1967: Cloud droplet growth by collection. *J. Atmos. Sci.*, **14**, 688–701.

——, and R. L. Reinhardt, 1974: An analysis of cloud drop growth by collection: Part I. Double distributions. *J. Atmos. Sci.*, **31**, 1814–1824.

Carroz, J. W., P. St. Amand and D. R. Cruise, 1972: The use of highly charged hygroscopic drops for fog dispersal. *J. Wea. Mod.*, **4**, No. 1, 54–69.

Cochet, R., 1952: L'évolution d'une gouttelette d'eau chargée dans un nuage à temperature positive. *Ann. Geophys.*, **8**, 33–54.

Davis, M. H., 1964: Two charged spherical conductors in a uniform electric field: Forces and field strength. *Quart. J. Mech. App. Math.*, **17**, 499–511.

——, and J. D. Sartor, 1967: Theoretical collision efficiencies for small cloud droplets in Stokes flow. *Nature*, **215**, 1371–1372.

Fletcher, N. H., 1962: *The Physics of Rainclouds.* Cambridge University Press, 386 pp.

Golovin, A. M., 1963: The solution of the coagulation equation for cloud droplets in a rising air current. *Bull. Acad. Sci. USSR, Geophys. Ser.*, No. 5, 783–791.

Gourdine, M. C., G. B. Carvin and A. Browne; 1974: EGD Fog Dispersal System Scaling Laws. *Preprints Fourth Conference on Weather Modification*, Ft. Lauderdale, Fla., Amer. Meteor. Soc., 264–270.

Goyer, G. G., J. E. McDonald, R. Baer and R. R. Braham, Jr., 1960: Effects of electric fields on water droplet coalescence. *J. Meteor.*, **17**, 442–445.

Jiusto, J. E., 1974: Remarks on visibility in fog. *J. Appl. Meteor.*, **13**, 608–610.

Johnson, D. B., 1972: Visibility calculations for microphysical computer models. Tech. Note No. 5–72, Environmental Prediction Research Facility, 23 pp. [DDC or NTIS AD776-228].

Kovetz, A., and B. Olund, 1969: The effect of coalescence and condensation on rain formation in a cloud of finite vertical extent. *J. Atmos. Sci.*, **26**, 1060–1065.

Levin, Z., M. Neiburger and L. Rodriguez, 1973: Experimental evaluation of collection and coalescence efficiencies of cloud drops. *J. Atmos. Sci.*, **30**, 944–946.

Lindblad, N. R., and R. G. Semonin, 1963: Collision efficiency of cloud droplets in electric fields. *J. Geophys. Res.*, **68**, 1051–1057.

Paluch, I. R., 1970: Theoretical collision efficiencies of charged cloud droplets. *J. Geophys. Res.*, **75**, 1633–1640.

Pauthenier, M., 1950: Electrical coalescence of fog and clouds. *Royal Meteorological Society, Centenary Proceedings*, 60–61.

Plumlee, H. R., and R. G. Semonin, 1965: Cloud droplet collision efficiency in electric fields. *Tellus*, **17**, 356–364.

Rayleigh, Lord, 1879: The influence of electricity on colliding water drops. *Proc. Roy. Soc. London*, **28**, 406–409.

Reinking, R. F., 1975: Project foggy cloud VII–warm fog dispersal and prevention (preliminary summary). NWC Tech. Memo. 2527, Naval Weapons Center, China Lake, Calif. 30 pp.

Sartor, D., 1954: A laboratory investigation of collision efficiencies, coalescence and electrical charging of simulated cloud droplets. *J. Meteor.*, **11**, 91–103.

——, 1960: Some electrostatic cloud-droplet collision efficiencies. *J. Geophys. Res.*, **65**, 1953–1957.

——, and C. E. Abbott, 1968: Charge transfer between uncharged drops in free fall in an electric field. *J. Geophys. Res.*, **73**, 6415–6423.

Scott, W. T., 1968: Analytical studies of cloud droplet coalescence. *J. Atmos. Sci.*, **25**, 54–65.

Shafrir, U., and M. Neiburger, 1963: Collision efficiencies of two spheres falling in a viscous medium. *J. Geophys. Res.*, **68**, 4141–4148.

Smith, M. H., 1972: Fog modification by means of electrified droplets. *J. Wea. Mod.*, **4**, 70–84.

Smith, T. B., C. W. Chien, and A. I. Weinstein, 1970: Warm fog modification. Final Rept., AFCRL-70-0105, Meteorology Research, Inc., Altadena, Calif., 52 pp.

Tag, P. M., 1971: Results generated from a one-dimensional warm fog model which simulates hygroscopic seeding. Navy Weather Res. Facility, Norfolk, Va. Tech. Paper No. 11–71, 63 pp. [DDC or NTIS AD769-226].

Whelpdale, D. M., and R. List, 1971: The coalescence process in raindrop growth. *J. Geophys. Res.*, **76**, 2836–2856.

Wobus, H. B., F. W. Murray and L. R. Koenig, 1971: Calculation of the terminal velocity of water drops. *J. Appl. Meteor.*, **10**, 751–754.